Heterogeneous pHPMA hydrogel promotes neuronal differentiation of bone marrow derived stromal cells *in vitro* and *in vivo*

To cite this article: Oksana Rybachuk *et al* 2023 *Biomed. Mater.* **18** 015027

IOP Publishing Biomed. Mater. 18 (2023) 015027 https://doi.org/10.1088/1748-605X/acadc3

Biomedical Materials

OPEN ACCESS

RECEIVED
27 June 2022

REVISED
27 November 2022

ACCEPTED FOR PUBLICATION
21 December 2022

PUBLISHED
4 January 2023

PAPER

Heterogeneous pHPMA hydrogel promotes neuronal differentiation of bone marrow derived stromal cells *in vitro* and *in vivo*

Oksana Rybachuk[1,2,*], Natalia Savytska[1,3], Éric Pinet[4], Yurii Yaminsky[5] and Volodymyr Medvediev[1,6]

[1] Bogomoletz Institute of Physiology NAS of Ukraine, Kyiv, Ukraine
[2] Institute of Genetic and Regenerative Medicine, M. D. Strazhesko National Scientific Center of Cardiology, Clinical and Regenerative Medicine, NAMS of Ukraine, Kyiv, Ukraine
[3] German Center for Neurodegenerative Diseases, Tübingen, Germany
[4] Resonetics, Québec, Canada
[5] State Institution 'Romodanov Neurosurgery Institute, NAMS of Ukraine', Kyiv, Ukraine
[6] Bogomolets National Medical University, Kyiv, Ukraine
[*] Author to whom any correspondence should be addressed.

E-mail: rbk@biph.kiev.ua

Keywords: bone marrow derived stromal cells (BMSCs), *poly*-[N-(2-hydroxypropyl)-methacrylamide] (pHPMA), NeuroGel, injection, rehydration, spinal cord injury (SCI)

Abstract

Synthetic hydrogels composed of polymer pore frames are commonly used in medicine, from pharmacologically targeted drug delivery to the creation of bioengineering constructions used in implantation surgery. Among various possible materials, the most common are poly-[N(2-hydroxypropyl)methacrylamide] (pHPMA) derivatives. One of the pHPMA derivatives is biocompatible hydrogel, NeuroGel. Upon contact with nervous tissue, the NeuroGel's structure can support the chemical and physiological conditions of the tissue necessary for the growth of native cells. Owing to the different pore diameters in the hydrogel, not only macromolecules, but also cells can migrate. This study evaluated the differentiation of bone marrow stromal cells (BMSCs) into neurons, as well as the effectiveness of using this biofabricated system in spinal cord injury *in vivo*. The hydrogel was populated with BMSCs by injection or rehydration. After cultivation, these fragments (hydrogel + BMSCs) were implanted into the injured rat spinal cord. Fragments were immunostained before implantation and seven months after implantation. During cultivation with the hydrogel, both variants (injection/rehydration) of the BMSCs culture retained their viability and demonstrated a significant number of Ki-67-positive cells, indicating the preservation of their proliferative activity. In hydrogel fragments, BMSCs also maintained their viability during the period of cocultivation and were Ki-67-positive, but in significantly fewer numbers than in the cell culture. In addition, in fragments of hydrogel with grafted BMSCs, both by the injection or rehydration versions, we observed a significant number up to 57%–63.5% of NeuN-positive cells. These results suggest that the heterogeneous pHPMA hydrogel promotes neuronal differentiation of bone marrow-derived stromal cells. Furthermore, these data demonstrate the possible use of NeuroGel implants with grafted BMSCs for implantation into damaged areas of the spinal cord, with subsequent nerve fiber germination, nerve cell regeneration, and damaged segment restoration.

1. Introduction

Synthetic hydrogels are hydrophilic porous polymers with a complex tertiary structure that are widely used in medicine to harboring and deliver pharmacologically active compounds, as well as for transplant bioengineering (Alfurhood *et al* 2017, Ghosh *et al* 2018, Lu *et al* 2018, Wang *et al* 2018, Li *et al* 2019).

As recent studies show, such synthetic hydrogels are hydroxyethyl cellulose hydrogel, polyacrylamide, polyacrylamide hydrogel, hydroxyethylcellulose hydrogel, which are used for knee pain in osteoarthritis; polyacrylonitrile hydrogel is used in degenerative disc disease; polyacrylamide hydrogel is used for urinary and anal incontinence (Mohapatra *et al* 2021).

For the delivery of active compounds, for example, doxorubicin, the following hydrogel variants are used: dual thermo- and pH-sensitive injectable hydrogels of chitosan/(poly(N-isopropylacrylamide-co-itaconic acid), pH-sensitive injectable-polysaccharide-based self-healing hydrogels, pH-responsive injectable hydrogels with mucosal adhesiveness based on chitosan-grafted-dihydrocaffeic acid and oxidized pullulan (Xie *et al* 2015, Qu *et al* 2017, Fathi *et al* 2019, Mohapatra *et al* 2021).

Hydrogels based on polyglycolic acid and polylactic acid are generally used in orthopedic practice, based on polylactide-co-glycolide or polyethylene glycol (PEG) for developments of different surgical materials (Cascone and Lamberti 2020).

The mammalian central nervous system possesses a low regenerative potential that manifests itself in limited neurogenesis (Becker *et al* 2018, Augusto-Oliveira *et al* 2019, Obernier and Alvarez-Buylla 2019, Snyder 2019) and long axonal connection revival. Decreased axonal regeneration in spinal cord injury (SCI) is caused by the apoptotic elimination of neuronal bodies, inhibition oligodendroglial proliferation in the traumatic injury zone, compact scar formation, and local expression of axonal growth cone repellents, such as leftover myelin, chondroitin sulfate proteoglycans, and a number of neurotrophic factors (Nishio *et al* 2018, Tran *et al* 2018, Yu and Gu 2018, Swieck *et al* 2019). In cases of severe traumatic SCI accompanied by spatial defects of nervous tissue, reconstructive surgery should utilize matrix transplant material that would support functional regeneration of the neural networks and fill in the traumatic injury site, restraining local inflammation and enabling transverse axonal outgrowth (Liu *et al* 2018, Wang *et al* 2018, Cizkova *et al* 2019, Liu *et al* 2019, Zhang *et al* 2019, Tashiro *et al* 2022, Wang *et al* 2022). Therefore, transplantation should prevent glial scar formation and support endogenous regeneration.

In general, materials of different origin are used for tissue engineering and reconstructive surgery—biological/natural (allografts and xenografts), synthetic (absorbable, permanent and mixed) and hybrid (bioglass). Matrices of different design/-structure are also used: 2D and 3D printed scaffolds, nanofibers and hydrogels (natural and/or synthetic) (Sharma *et al* 2019, Lv *et al* 2022). The matrix systems most widely used in reconstructive surgery are classified into several groups based on their chemical nature: PEG derivatives, *poly*-[N-(2-hydroxypropyl)methacrylamide] (pHPMA), poly-ε-caprolactone, poly lactic acid, poly lactic-co-glycolic acid, poly-β-hydroxybutyrate, and polyvinyl derivatives (Wang *et al* 2018, Liu *et al* 2019, Zhang *et al* 2019, Cheng *et al* 2022). The application of PEG derivatives has recently been confirmed to have a number of serious disadvantages, such as complement system activation, rapid degradation in subsequent transplantations, and excessive oxidation (Alfurhood *et al* 2017). This makes the effectiveness of the PEG-based matrix implantation questionable. At the same time, pHPMA derivatives have been actively used in medicine for over 30 years, and in comparison with PEG, possess advantages, such as the capacity for functional modification of a derivative by modifying secondary hydroxyl residues (Kopecek and Kopecková 2010, Alfurhood *et al* 2017). Such modifications enable the enhancement of astroglial and axonal adhesion to transplant, which in turn improves their growth and structural regeneration of the tissue hydrophilic polymer macromolecules capable of swelling in aqueous solutions. However, it is important to note that the hydrophilic structure of synthetic hydrogels has the potential risk of excessive swelling of the introduced transplant, which in turn, may lead to additional compression (secondary injury) of the damaged spinal cord. This property should be considered in both animal experiments and clinical trials (Rustagi and Lavelle 2014, Dietz and Schwab 2017).

One such pHPMA derivative is NeuroGel, a biologically compatible hydrogel whose distinctive structure supports a chemically stable and physiological environment when in contact with the nervous tissue necessary for the recipient cells to grow. This hydrogel has pores of varying diameters (2 nm–300 μm) that allow macromolecules, cellular processes, and whole cells to migrate through the transplant (including vasculature outgrowth) (Woerly *et al* 2001a, 2001b, 2005). Even though this polymer is not biodegradable, its high hydration capacity (the mass of water in the intact sample reaches 96%) allows for the substitution by bioactive molecules in the process of the endogenous regeneration and transverse outgrowth of the living tissue inside the gel (Kopeček and Bažilová 1973, Bohdanecky *et al* 1974, Kopecék and Baźilová 1974, Woerly *et al* 1998, Woerly *et al* 2001a). As shown by the previously studied physicochemical properties (Woerly *et al* 1998, 1999), the pHPMA hydrogel has not only a high water content, but also a high fractional porosity (hyperporous structure). The viscoelastic properties of the hydrogel provide complete sealing of the tissue defect in terms of volume and shape (Woerly *et al* 1998, 1999). Using infrared microscopy, it was shown that the surface of the hydrogel is the site of protein and lipid adsorption (Woerly *et al* 1998, 1999). Active NeuroGel testing has proven the absence of cytotoxicity, neurotoxicity, chronic toxicity, mutagenicity, and pyrogenicity of the material. In addition, this hydrogel possesses long-term chemical and thermal stability that enables sterilization of NeuroGel by means of ordinary autoclaving. Porous structures allow biological macro- and micromolecules and ions to freely diffuse into the gel (Sprincl *et al* 1976,

Říhová et al 1985, Woerly et al 1993, 1996, 1999). Another recently introduced therapeutic approach for SCI treatment is the transplantation of stem cells originating from various sources with the purpose of enhancing regeneration, countering inflammation, and facilitating possible transplanted cell differentiation and reconstitution of the recipient's lost tissue (Lu et al 2017, Nori et al 2017, Wang et al 2018, Cizkova et al 2019, Shah et al 2020, Farid et al 2022, Suzuki et al 2022). However, interventions designed in this manner have a meek positive effect in clinical trials (Verstappen et al 2022), although some studies have indicated their statistical significance (Myers et al 2016, Fan et al 2017). Results of meta-analysis dedicated to mesenchymal stem cell (MSC) and progenitor transplantation in experimental SCI (Oliveri et al 2014, Zhang and He 2014), provide evidence for the positive outcome of the procedure and ∼15% recovery of the normal locomotor hind limb function in rats, according to Basso–Beattie–Bresnahan (BBB) assessment. Long-term outcomes were estimated to be modest (Oliveri et al 2014, Badner et al 2017) in particularly because of the low level of cell survival in the large injury area (Tetzlaff et al 2011, Vismara et al 2017).

Thus, the effective combination of these two strategies in restorative surgery, i.e. the creation of biohybrid systems, holds great promise for enhanced morphological and functional regeneration of nervous tissue (Liu et al 2018, Wang et al 2018, Cizkova et al 2019, Liu et al 2019, Zhang et al 2019, Tashiro et al 2022, Wang et al 2022).

The number of studies dedicated to hydrogels, in particular pHMPA derivatives seeded with different types of cells, including stem types, is currently very limited (Badner et al 2017, Liu et al 2019, Zhang et al 2019), which creates a gap in the knowledge on how the synthetic matrix affects cell potency, proliferative status, phenotype, mitotic activity and differentiation capacity under conditions of first-order contact or long-term survival within the depth of the artificial matrix. However, there are currently no studies on the regenerative potential of pHPMA hydrogel (NeuroGel) associated with stem cells or their derivatives against the background of SCI. Therefore, we assessed the properties of bone marrow stem/stromal cells (BMSCs) after cultivation with NeuroGel and the effectiveness of using such a biofabricated system on a model of SCI in rats.

Combining these two novel techniques would improve the outcomes of spinal cord restorative therapy by inhibiting the secondary inflammatory response, providing an environment for nervous fiber remyelination, and stimulating their regenerative outgrowth through the traumatic injury region. Furthermore, it will not only support the endogenous regenerative process or mechanical spinal cord reconstruction, but also enhance endogenous regeneration and prevent inflammation from spreading, as well as promote restoration of the lost reflexive, motor, and sensory functions of the spinal cord.

2. Materials and methods

2.1. Characteristics of pHPMA hydrogel

For this experimental reconstructive surgery, we chose polymer hydrogel NeuroGel (Type I, Model NG-5). NeuroGel is a synthetic microporous highly hydrated hydrogel composed of *poly*-[N-(2-hydroxypropyl)-methacrylamide] synthesized by É. Pinet laboratory (*Aqua Gel Technologies, Canada*) from N-(2-hydroxypropyl) methacrylamide (Kopeček and Bažilová 1973, Bohdanecky et al 1974, Kopecék and Baźilová 1974) under heterophase separation conditions and nitrogen as a gas phase by means of radical polymerization in a pore forming solvent with divinyl transverse bonds formation (Woerly et al 1998). Hence, NeuroGel is a completely synthetic polymer of class III neurodevices. Structurally, the pores in this hydrogel were classified as macropores, micropores, and nanopores, with diameters ranging from 2 nm to 300 μm. The structure of the major hydrogel component consists of aggregated polymer microspheres, which allow for the variation in the diameter of the porous complex in combination with an increased surface area suitable for cellular adhesion.

2.2. Bone marrow stem/stromal cell isolation and cultivation

Bone marrow cells were obtained from three-month-old Green Fluorescent Protein (GFP)-positive Friend leukemia virus B (FVB) mice ($n = 3$) by flushing the femurs with Roswell Park Memorial Institute (RPMI-1640) medium (Sigma, USA) under sterile conditions. Cells were seeded on 25 cm^2 flask 100 mm^{-1} Petri dishes at a density of 4×10^5 cells cm^{-2} and cultured for 2 weeks in culture medium, which change every 2–3 d. Cells were cultured in a humid CO_2-incubator with 5% CO_2 in the air at +37 °C. Cells were first passaged at the 80% confluency of the monolayer. To achieve this, cells have been detached from the surface of the flask with 0.02% Trypsin-EDTA (Sigma, USA) and transferred to the new flasks for seeding at 2×10^4 cells cm^{-2} density. For the second passage, BMSCs were seeded onto the 4-well plates at a density of 3×10^4 cells/well and cultivated for another 14 d. For co-culture with the hydrogel and injection into the hydrogel, 2nd passage BMSCs were used (figure 1(a)).

Standard conditions were applied for the BMSC culture. BMSCs culture medium had the following content: 42.5% RPMI-1640 (Sigma, USA); 42.5% Dulbecco's Modified Eagle Medium (DMEM) (Sigma, USA), 15% FBS (Sigma, USA), 2 mM L-glutamine (HyClone, Ireland), and 1% penicillin/streptomycin (Gibco, Canada).

2.3. BMSCs phenotyping

The percentage of viable BMSCs in the suspension was determined by flow cytometry (FACS Aria, Becton Dickinson, USA) after incubation of the cell suspension with 7-aminoactinomycin (7-AAD). Phenotyping of 2nd passage BMSC cultures ($n = 3$) was performed to investigate the expression of surface markers specific to mesenchymal stromal cell culture, namely, CD44, CD73, CD90 positive, CD34, CD45, and CD117 negative. To achieve this goal, we used monoclonal antibodies conjugated with fluorochromes, in accordance with the manufacturer's recommendations (Becton Dickinson, USA). 2×10^5 cells in 50 µl of RPMI-1640 (Sigma, USA) were incubated with corresponding monoclonal antibodies at 1:50 dilution (0.5 µg/10^6 cells) in the 5 ml polystyrene tubes. Cells were incubated with antibodies for 30 min at +4 °C protected from light, then 1 ml *CellWash* (Becton Dickinson, USA) buffer was added, and the resulting mixture was centrifuged at 300 × *g* for 5 min at +4 °C. Supernatant was removed, and the pellet was resuspended in 300 µl of phosphate buffer saline (PBS) (Sigma, USA) supplemented with 1% BSA (Sigma, USA). Immediately before analysis, the suspension was filtered through a cell strainer with a pore diameter of 70 µm. Analysis was performed on a BD FACS Aria cell sorter (Becton Dickinson, USA), using BD FACS Diva 6.1 software. To adjust compensation for fluorochrome emission spectrum overlap during the multiparametric analysis, unstained controls, single-stained controls, and fluorescent minus one control were used. A minimum of 1×10^4 cells were counted per tube. The viability and level of surface marker expression was measured as a percentage and statistically calculated using the Mann–Whitney *U*-test.

2.4. Directed osteogenic and adipogenic differentiation of BMSCs

Osteogenic differentiation of BMSCs was induced according to the protocols described by (Matsuda *et al* 2005, Li *et al* 2009, Bianco *et al* 2010, Can and Balci 2011). For directed osteogenic differentiation, the cells were seeded in 35 mm Petri dishes at a concentration of 4×10^5 in complete growth medium. 24 h later, the growth medium was changed to osteogenic medium that consisting of DMEM low glucose (1 g l^{-1}) (Sigma, USA) supplemented with 10% FBS (Sigma, USA), L-ascorbic acid 2-phosphate (0.05 mM) (Sigma, USA), dexamethasone (100 nM) (Sigma, USA), and β-glycerophosphate (10 nM) (Sigma, USA). The osteogenic medium was changed every 3–4 d. Osteogenic differentiation took 21 d under normal culture conditions. After 21 d, the cell monolayer was washed with PBS (Sigma, USA) and fixed with cooled 10% formalin solution (Sigma, USA) solution for 20 min. Fixed cell monolayer was stained with 2% solution of Alizarin Red S (Sigma, USA) for calcium salt deposit detection in the extracellular matrix. Analysis of mineralization in Alizarin red-stained cultures was performed visually using a microscopy (Olympus BX51, Japan). After induction, the cultures were stained for alkaline phosphatase (ALP). For the identification of ALP activity, the BCIP/NBT Liquid Substrate System (Sigma, USA) was used.

For directed adipogenic differentiation, BMSCs were seeded into 35 mm Petri dishes at a density of 4×10^5 in the growth medium. After 24 h, the growth medium was changed to an adipogenic medium that consisted of high glucose (4.5 g l^{-1}) DMEM (Sigma, USA) supplemented with 10% FBS (Sigma, USA), 1 µM dexamethasone (Sigma, USA), 200 µM indomethacin (Sigma, USA), 500 µM 3-isobutyl-1-methylxanthine (Sigma, USA), and 5 µg ml^{-1} insulin (Sigma, USA). The fresh adipogenic medium was changed every 3–4 d. Adipogenic differentiation required 14 d under standard culture conditions. After 14 d, the cells were washed with phosphate buffer and fixed in the ice-cold 10% paraformaldehyde solution (Sigma, USA) for 20 min. The fixed cells were then stained with 5% Oil Red O solution (Sigma, USA) for the detection of lipid inclusions. The stained cells were visually assessed for lipid inclusions within ten random fields of view using a microscope (Olympus BX51, Japan).

2.5. BMSCs and hydrogel co-culture methods

Immediately before the co-culturing procedures and BMSCs injection into the hydrogel/NeuroGel fragments (HGI-group), the fragments were partly rehydrated (HGII-group) with a small amount of culture medium solution. The co-culture of BMSCs with the hydrogel (biofabrication system) was initiated by either direct injection (for maximum populating of the hydrogel with cells) using a syringe (five punctures) of the cell suspension (50 µl, 3×10^4 cells) into the rehydrated fragment (14 mm^3) or superficial rehydration of 14 mm^3 fragments with cell suspension (50 µl, 3×10^4 cells). The hydrogel fragments containing cells were placed into 4-well plates with the culture medium for BMSCs. In both methods, BMSCs were cultured with NeuroGel for 14 d. BMSCs were cultured without hydrogel (control cultures) in the same medium as with hydrogel and for the same time.

2.6. Immunostaining of BMSCs after co-cultivation with hydrogel

Fragments of hydrogel co-cultured with BMSCs and were fixed in 4% paraformaldehyde solution (Sigma, USA); hydrogel fragments were sectioned into 50 µm thick slices using automatized vibratome LeicaVT1000A (Leica, Germany). Slices were then treated with blocking solution (0.3% Triton X-100 (Sigma, USA) and 1% BSA (Sigma, USA)) for non-specific binding prevention and improve of antibody penetration into the samples. The preparations were

incubated with a mixture of primary antibodies for 24 h. For BMSCs (in particular within the hydrogel fragments after injection and rehydration), proliferating and differentiated neuronal-like cells identification double immunostaining was performed, using antibodies against GFP (1:1000, NB, UK), Ki-67 (1:200, Abcam, UK), NeuN (1:200, Abcam, UK), and β(III)-tubulin (1:500, Sigma, Germany). Nuclei were counterstained with the nucleic acid dye Hoechst 33342 (1:5000, Abcam, UK). After washing in 0.1 M PB, the sections were incubated for 2 h with a mixture of secondary antibodies anti-goat-Alexa Fluor-488 (1:1000, Invitrogen, USA), anti-mouse-Alexa Fluor-555 (1:1000, Invitrogen, USA), and anti-rabbit-Alexa Fluor-647 (1:1000, Invitrogen, USA).

Cell cultures and hydrogel sections with BMSCs were mounted with Fluoromount™ Aqueous Mounting Medium (Sigma, USA) under a cover glass and analyzed visually using a FluoView™ FV1000 confocal microscope (Olympus Inc., Japan) with a camera connected to a computer.

2.7. Surgery for spinal cord hemisection and implant embedding

Sixteen adult (4–4.5 months, ∼250 g) white outbreeding male rats on the base Wistar were used to induce spinal cord hemisection. SCI was modeled under general anesthesia (by intra-abdominal injection of xylazine 15 mg kg^{-1} (Biowet, Poland) and ketamine 70 mg kg^{-1} (PJSC 'Farmak', Ukraine)) after reaching a state of deep muscle relaxation, the absence of corneal reflexes and preserving voluntary breathing of the animal in moderate aseptic conditions. As previous shown (Kopach *et al* 2017, Medvediev *et al* 2021), the caudal edge of the chest of a deeply anesthetized animal was determined by palpation, without the use of additional microsurgical or radiological imaging. This, given the theoretically greater mobility of the last pairs of ribs, provides for localization of the laminectomy and SCI region, most probably on the level of spinal cord segments T_{13}–L_1 (for detail (Medvediev *et al* 2021)). After laminectomy, the spinal cord was perforated parasagitally in the dorsoventral direction using an insulin syringe. One of the branches of ophthalmic scissors was introduced into the channel. The second branch covered the left half of the spinal cord, together with the trunks of the sensitive roots, and was dissected in a few stages. The state of the dura mater within the bone window was not determined, and the spinal cord was not separated from the adjacent nerve stems before SCI modeling. Blind mechanical control of the completeness of the cross-section of half the diameter of the spinal cord was performed using ophthalmic tweezers curved along the rib, rigidly passing its working end along the inner surface of the *vertebral* canal in the area of injury. After spontaneous cessation of bleeding, the SCI cavity was filled with a preliminarily prepared hydrogel implant. All hydrogel fragments were incubated with BMSCs for 14 d prior to implantation. After implantation, the bone window to the vertebral canal was covered with a subcutaneous connective tissue fragment, the soft tissues and skin were sutured, and the injured area was treated with povidone-iodine solution (EGIS; Hungary). A bicylline-5 solution (PJSC Kyivmedpreparat, Ukraine) was subcutaneously administered into the posterior cervical region at a dose of ∼0.6 × 10^6 U kg^{-1} of live weight. A dexamethasone solution (KRKA, Slovenia) was intra-abdominally injected at a dose of ∼6 mg kg^{-1} of live weight as an anti-inflammatory and anti-edematous therapy. After the operation and until complete awakening, the animals were kept under increased air temperature. Subsequently, the animals were returned to individual cages at 22 °C–25 °C in light controlled rooms (2/12 h light/dark cycle) and fed *ad libitum* for approximately 7 months (28 weeks) before they were perfused.

2.8. Spinal tissue preparation and tissue immunostaining

To evaluate the effect of the implants on nerve tissue recovery, spinal cords were harvested approximately seven months post-surgery. Animals were perfused transcardially with isotonic physiological saline followed by 4% paraformaldehyde (Sigma, USA) under deep anesthesia.

The area of the spine, which included the area of the SCI, was removed, and placed in a 4% paraformaldehyde solution (Sigma, USA). After approximately one week, the spinal cord was isolated by micropreparation, the caudal and rostral areas were cut off with a blade, fixed in the 4% paraformaldehyde (Sigma, USA) for 24 h, and then placed into PBS (Sigma, USA) at 4 °C. Next, spinal cords were placed in a 2% agarose solution, kept for 5–7 min at 4 °C and were cut into 50–60 μm thickness longitudinal sections of spinal cord (each animal) using a vibratome (Leica VT 1000A, Germany). For immunostaining, vibratome sections of spinal cord around the injured site and implanted hydrogel with BMSCs were washed three times in PBS (Sigma, USA), permeabilized with 0.3% Triton X-100 (Sigma, USA) and incubated for 2 h with 1% BSA (Sigma, USA).

Following the sections of spinal cord were incubated overnight at 4 °C with primary antibodies as follows: GFP (1:1000, NB, UK), Glial fibrillary acidic protein (GFAP) (1:500, Sigma, USA), β(III)-tubulin (1:500, Sigma, Germany) followed by incubation with Alexa 488 conjugated donkey anti-goat secondary antibodies (1:1000, Invitrogen, USA) and Alexa 555 conjugated donkey anti-mouse secondary antibodies (1:1000, Invitrogen, USA), and Alexa 647 conjugated donkey anti-rabbit secondary antibodies (1:1000, Invitrogen, USA) for 2 h at room temperature. Nuclei

were labeled with Hoechst 33342 (1:5000, Abcam, UK). All images were collected using a FluoView™ FV1000 confocal microscope (Olympus Inc., Japan).

2.9. Data analysis

Statistical analyses were performed using statistical software (version 5, StatSoft, Tulsa). Data are presented as mean ± standard error of the mean. Student's two-tailed t-test was used for the comparative evaluation of the means obtained. The difference between means was considered significant at $p < 0.05$. Cell cultures growing in the presence of a hydrogel (with different population variants) were compared with each other and with a cell culture without hydrogel (control cell culture). In groups where cells were cultured inside the hydrogel, cell cultures of different population variants (injection or rehydration) were compared with each other.

For calculating a relative count of the Ki-67-positive cells and NeuN-positive cells in BMSCs culture (on the glass near the hydrogel and inside the hydrogel) before implantation to SCI, the following formula was used: % of Ki-67-positive cells = count of cells with the colocalized Hoechst-positive nuclei and Ki-67 marker/total count of Hoechst-positive cell nuclei; % of the NeuN-positive cell = count of cells with the colocalized Hoechst-positive nuclei and NeuN marker/total count of the Hoechst-positive cell nuclei. Cells were counted on the same hydrogel area (edge, middle and center) of each group. The data presented in the graphs are averaged values from different areas of the hydrogel fragment.

3. Results

3.1. BMSCs isolation, cultivation and phenotyping

The stem cell source was the bone marrow of 3-month-old FVB GFP transgenic mice. Percentage of viable BMSCs in the cell suspension estimated by flow cytometry was 95.2% ± 1.9% ($n = 3$). When cultivated, BMSCs showed inherent adhesive ability and fibroblast-like morphology (figure 1(a)).

Immunophenotyping of BMSC cultures ($n = 3$) at two passages revealed relatively high expression of CD44 (91.3% ± 2.5%), moderate for CD90 (29.9% ± 24.3%) and CD73 (14.6% ± 3.6%) markers, and low expression of CD34 (2.1% ± 0.8%) marker, which is a characteristic expression pattern of the multipotent cells. However, for a long period, the cells had also maintained expression of CD45 (48.2% ± 11.8%) and CD117 (36.1% ± 4.5%). Mouse BMSCs cultures are known to consist of heterogeneous cell populations that highly express CD45 during early passages. Hence, the culture obtained for the experiment, fulfills the minimal criteria of MSCs including the phenotype and its ability of multilineage differentiation (Dominici *et al* 2006, Ooi *et al* 2008).

3.2. BMSCs osteogenic and adipogenic differentiation potential

Visual assessment of the stained culture with microscopy revealed depositions of Alizarin Red S in the extracellular matrix, which confirms the ability of the cultured cells to differentiate into the osteogenic lineage (figure 1(c)). Meanwhile, treatment of cells with the ALP substrate BCIP/NBT Liquid Substrate System (Sigma, USA) confirmed the high enzymatic activity of ALP in the cells (figure 1(d)) as a marker of osteoinduction.

Multiple lipid inclusions were revealed in the cell culture after staining with Oil Red O solution (figure 1(b)). This confirms that the ability of BMSCs to differentiate in the adipogenic direction.

3.3. Immunostaining and quantitative analysis of BMSCs cultures cultivated near the hydrogel (on the glass) and hydrogel fragments seeded with BMSCs

Immunocytochemistry was used not only to detect the presence of BMSCs, but also to detect changes in proliferation both in culture (on the glass near the hydrogel) and within the hydrogel fragments.

BMSCs co-cultured with the hydrogel (on the glass near the hydrogel) for 14 d by both methods (as well as control cells cultivated without hydrogel) manifested a high number of Ki-67-positive cells, which indicated preservation of their proliferative activity (figures 2(a) and (c)–(ci)). Ki-67 is proliferation marker that localizes on the cell surface during interphase, whereas during mitosis, it is bound to chromosomes.

The percentage of Ki-67-positive cells after co-cultivation with hydrogel (on the glass near the hydrogel) amounted to 25.4% ± 2.3% ($n = 10$) (injection method) and 28.9% ± 3.2% ($n = 10$) (rehydration method), while in control cultures it reached 30.1% ± 4.2% ($n = 10$) of the total number of cells (total number of cells = 100%, Hoechst-positive cell nuclei) (figure 2(b)).

After 14 d of co-cultivation, the BMSCs in the hydrogel fragments preserved their viability, while the relative number of Ki-67-positive cells in comparison with the initial culture was lower (figures 2(c) and (ci); figures 3(b) and (bi)).

For the cells injected into hydrogel, only 13.7% ± 2.2% ($n = 11$) were Ki-67-positive, while for the rehydration, that number amounted to 18.6% ± 5.6% ($n = 5$) (figure 3(d)).

Notably immunostaining revealed no NeuN-positive cells; thus, no neuronal differentiation was observed in the BMSC cultures cocultivated with (on the glass near the hydrogel) hydrogel fragments (data not shown). No positive NeuN staining was observed in BMSC cultures (control cultures) cultivated without hydrogel (data not shown).

However, in the BMSCs inside the fragments of the hydrogel, both after injection and

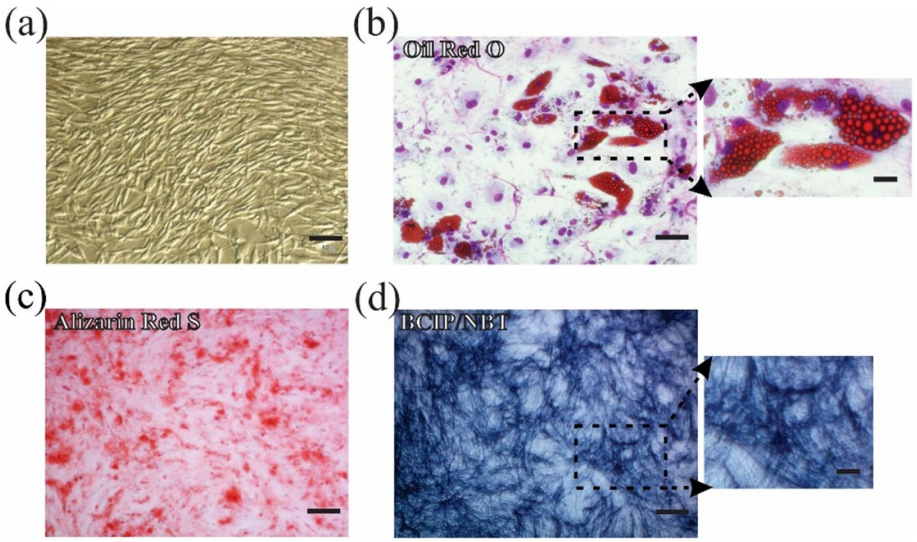

Figure 1. Characterization of BMSCs. (a) The morphology of BMSCs from passage 2, scale bar 70 μm. (b) Oil red O stained lipid droplets were observed in cytoplasm after adipogenic induction for 14 d, scale bar 40 μm, insert 10 μm. (c) Alizarin red S stained mineralization nodules were observed in matrix after osteogenic induction for 21 d, scale bar 70 μm. (d) ALP activity in BMSCs after osteogenic induction for 21 d, scale bar 70 μm, insert 20 μm.

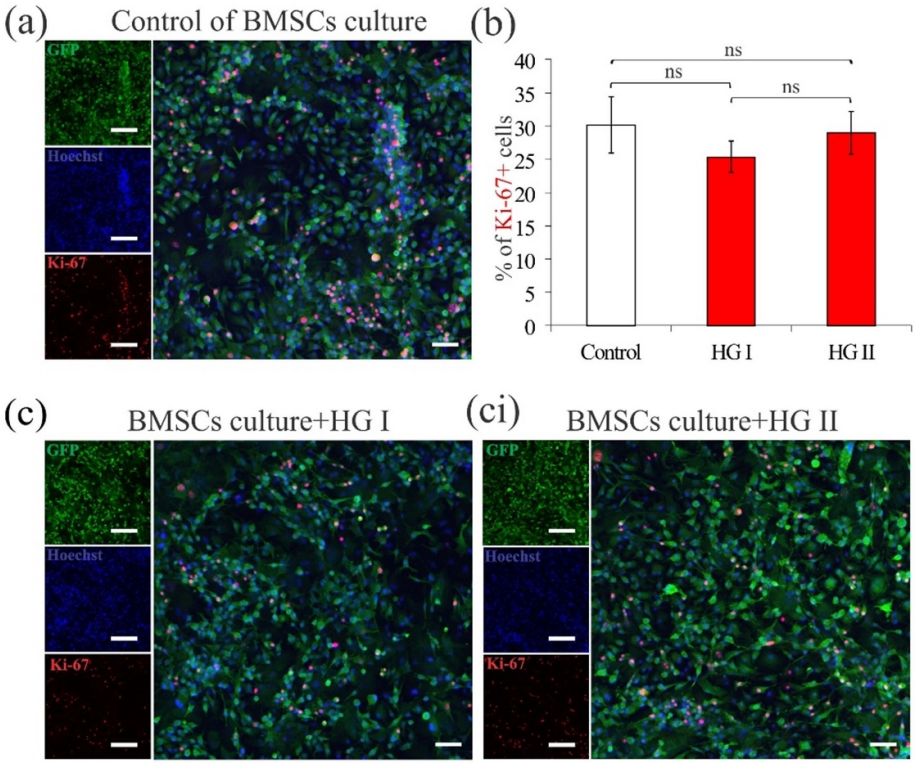

Figure 2. Proliferative activity of BMSCs after cultivation (14 d) with hydrogel (on the glass near the hydrogel). (a), (c) and (ci)—Representative confocal images of BMSCs after 14 d of cultivation stained for GFP (green), Ki-67 (red) and Hoechst (blue). (a)—control culture, without hydrogel. (c), (ci)—BMSCs after cultivation with hydrogel: BMSCs culture + HGI—variant of injection, BMSCs culture + HGII—variant of rehydration, scale bars 150 μm, merge 50 μm. (b)—Percentage of the Ki-67-positive BMSCs after different variants of cultivation with hydrogel; Student's two-tailed *t*-test; ns–no significant difference between groups.

rehydration, the quantity of the NeuN-positive cells amounted to 63.5% ± 3.1 (n = 23) and 57.0% ± 5.3 (n = 11), respectively (figure 3(e)). The obtained results indicate that BMSCs inside the hydrogel are capable of differentiating into cells expressing typical neuronal markers such as NeuN and β(III)-tubulin (figures 3(c), (ci) and 4(a)–(ai)).

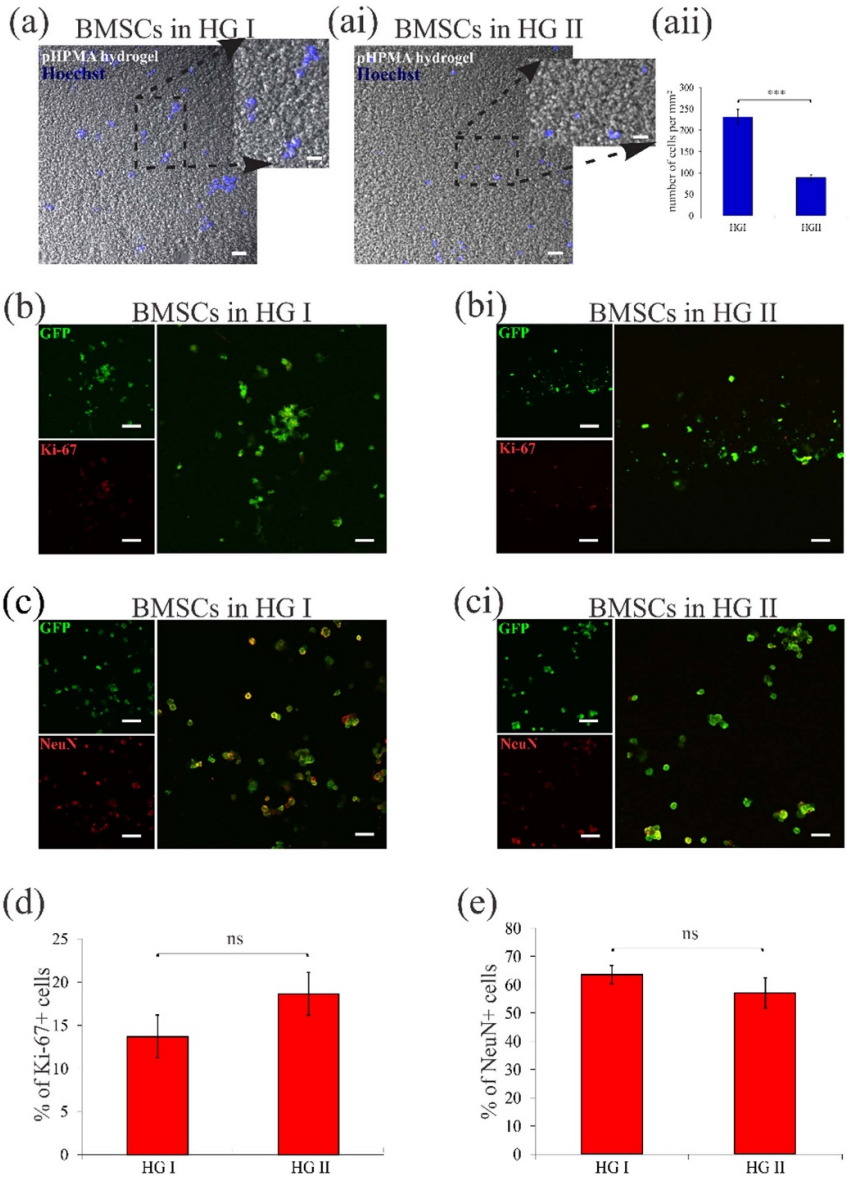

Figure 3. Identification of BMSCs in hydrogel fragments (14 d culturing) before implantation to SCI. (a), (ai)—Fragments of hydrogel with Hoechst-positive (blue) nuclei of BMSCs, (a)—variant of injection (HGI), (ai)—variant of rehydration (HGII); scale bars 50 μm, insert 20 μm. (aii) Quantitative analysis of cell nuclei per mm^2 of hydrogel; data are mean with SEM; Student's two-tailed *t*-test; $^{***}p < 0.001$. (b)–(ci) Representative confocal images of hydrogel fragments with BMSCs after 14 d of cultivation stained for GFP (green), Ki-67 (red (b), (bi)) and NeuN (red (c), (ci)); (b), (c)—variant of injection (HGI), (bi), (ci)—variant of rehydration (HGII). Scale bars 100 μm, merge 50 μm. (d) Percentage of the Ki-67-positive BMSCs in hydrogel fragments after 14 d culturing; ns–no significant difference between groups. (e) Percentage of the NeuN-positive BMSCs in hydrogel fragments after 14 d culturing; ns–no significant difference between groups.

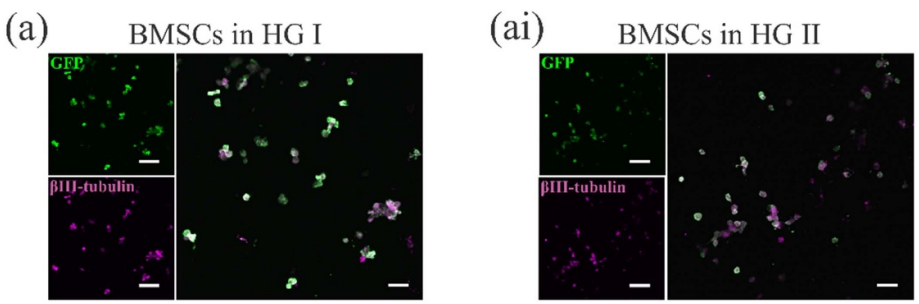

Figure 4. β(III)-tubulin identification of BMSCs in hydrogel fragments (14 d culturing) before implantation to SCI. (a)–(ai)—Representative confocal images of hydrogel fragments with BMSCs after 14 d of cultivation stained for GFP (green) an β(III)-tubulin (magenta); (a)—variant of injection (HGI), (ai)—variant of rehydration (HGII); scale bars 100 μm, merge 50 μm.

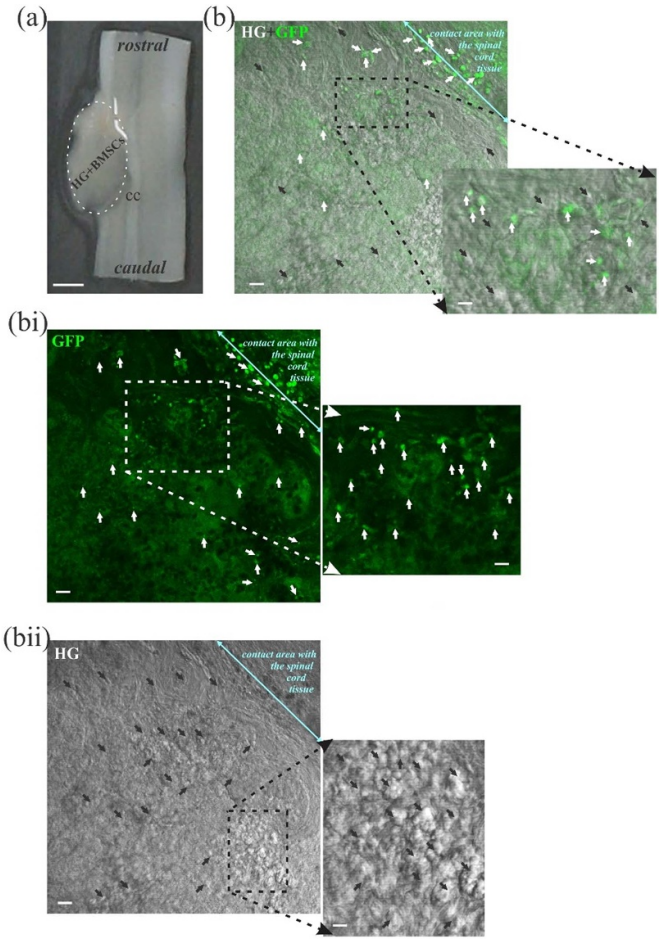

Figure 5. Investigation of implanted fragments (*in vivo*): the existence of BMSCs in hydrogel after implantation into the damaged rat spinal cord (∼7 months). (a)—spinal cord section with implant (NeuroGel + BMSCs), cc—central channel, scale bar 1 mm; (b)—fragment of hydrogel (HG) with GFP-positive (green, white arrows) BMSCs (like an implant in the rat spinal cord), black arrows are matrix pores, scale bars 30 μm, insert 12 μm. (bi)—GFP-positive cells (green, white arrows) in fragment of hydrogel, scale bars 30 μm, insert 12 μm. (bii)—fragments of hydrogel (HG) (stability of the matrix porous structure), black arrows are matrix pores; scale bars 30 μm, insert 12 μm.

It should be noted that in the variant of injectable populating of the hydrogel with cells, the BMSCs were placed in most cases evenly over the entire area of the hydrogel fragment. And in the case of rehydration of the hydrogel with a cell suspension, BMSCs filled the hydrogel over 70%–75% of its area: basically, the cells were concentrated along the edges of the hydrogel fragment. Instead closer to the center of the hydrogel fragment, either single cells were observed, or no cells were observed at all.

Quantification of the BMSCs by Hoechst-positive cell nuclei inside the hydrogel fragments showed that the number of cells after the injection was 231.3 ± 17.5 ($n = 34$), and the number of cells inside the hydrogel after rehydration reached 88.7 ± 6.2 ($n = 16$) ($p < 0.001$) cells per mm^2 of hydrogel (figures 3(a)–(aii)).

The obtained data suggest that both methods of BMSCs co-cultivation with hydrogels are suitable for further applications, such as transplantation/implantation into the brain or spinal cord.

3.4. Implantation of the hydrogel + BMSCs after SCI. General characteristics of the hydrogel + BMSCs *in vivo*

Fragments of implants (hydrogel + BMSCs) were immediately introduced into the rat spinal cord tissue after injury modeling. As a model of SCI, we used hemisection. The hemisection model provides technical simplicity, repeatability, low mortality rate against the background of severe ipsilateral deficiency of spinal cord function. Animals ($n = 16$) were kept under stable vivarium conditions (see Materials and methods) for approximately 7 months prior to perfusion with further immunostaining. It should be noted that during this period (∼7 months after SCI and implantation), all rats survived, and no spontaneous deaths were observed.

After a histological study of the rat spinal cord tissue with biofabricated inserts (hydrogel + BMSCs), it was found that this hydrogel was in very close contact with the damaged tissue of the spinal cord (figure 5(a)), and the nerve processes of the recipient

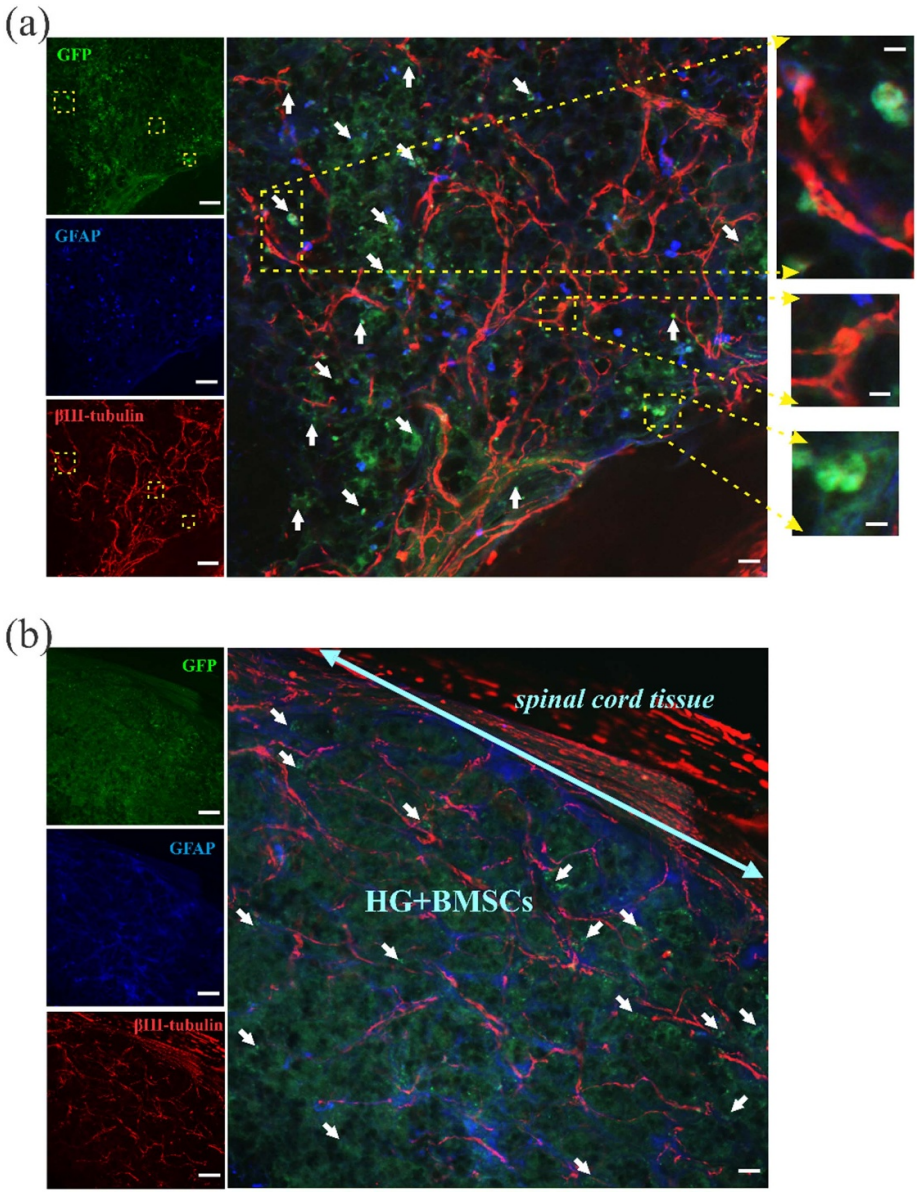

Figure 6. Neuroregenerative effect of implantation and identification of GFP$^+$-BMSCs in hydrogel fragments after implantation (∼7 months) into the damaged rat spinal cord. (a), (b)—representative confocal images of hydrogel fragments with BMSCs after implantation stained for GFP (green), GFAP (blue) and β(III)-tubulin (red); (a)—implant area: hydrogel + BMSCs; (b)—implant insertion area in the damaged spinal cord; white arrows indicate of GFP$^+$-cells; yellow boxes are GFP$^+$ β(III)-tubulin$^+$ cells; scale bars 70 μm, merge 25 μm, inserts 10 μm.

cells perfectly grew into the matrix. It was also shown that GFP-positive BMSCs were present not only in the hydrogel, but also in the contact zone with the spinal cord tissue (figures 5(b) and (bi)).

Since the cells are located in the contact zone of the hydrogel with the nervous tissue, we can assume a close functional interaction of these cells with the cells (outgrowths) of the recipient. NeuroGel itself, as a hydrogel matrix, retains its porous structure (figure 5(bii)) after implantation (∼7 months) in the damaged area of the spinal cord. These properties of the pHPMA hydrogel enable them to be seeded with stem cells, which can attach, survive, and grow inside the porosity of the hydrogel.

3.5. Immunostaining of spinal cord tissue with hydrogel + BMSCs

The following antibodies were used for immunostaining of the spinal cord tissue and the implant area: GFP, visualization of BMSCs in the hydrogel; β(III)-tubulin, a marker of neurons, including their processes; GFAP, a marker of astrocytes.

Approximately seven months after insertion into the damaged tissue of the rat spinal cord as part of the implants, a large number of GFP-positive cells (BMSCs) were observed, which were placed in the middle of the hydrogel (implant) (figure 6(a)) and near the zone of direct contact with the tissue of the recipient (figure 6(b)).

At the same time, the biofabricated implant (hydrogel + BMSCs) contained β(III)-tubulin-positive cells (their processes were quite clearly visible). These cells formed a dense network between themselves, both in the middle of the implant itself (hydrogel) (figure 6(a)) and in the contact zones (figure 6(b)) with the cells of the recipient's damaged tissue. Many β(III)-tubulin-positive cells were GFP-positive, and this gives us the right to state that the BMSCs in the hydrogel differentiated into neurons (figure 6(a) yellow boxes). The damaged tissue of the recipient tightly adhered to the contact zone of the implant, and that we did not notice a single gap between them.

In turn, using the astrocyte marker GFAP, these cells were found to be present in the implant (hydrogel + BMSCs). Astrocytes were evenly distributed over the entire area of the implant and at the points of contact between the implant and the recipient tissue. It should be noted that we did not observe the accumulation of astrocytes (a variant of glial scar formation) in the area of injury/implantation in any animal.

4. Discussion and conclusion

In contrast to other vertebrates, mammals possess limited Central nervous system (CNS) regeneration (Becker *et al* 2018, Augusto-Oliveira *et al* 2019, Obernier and Alvarez-Buylla 2019, Snyder 2019). However, after SCI (Khorasanizadeh *et al* 2019), mammals are capable of spontaneous recovery that heavily depends on the initiation of endogenous regenerative processes, that in turn, depend on the extracellular matrix or its qualitative substitution (Blesch and Tuszynski 2009, Domínguez-Romero and Slater 2021). Such substitutions should exhibit properties of the body's natural environment, especially its molecular and structural composition, enabling directed axonal growth and myelination. One of the most prominent causes of reduced spinal cord regeneration potential is the chronic expression of repellent factors at the injury site (Tran *et al* 2018, Yu and Gu 2018, Swieck *et al* 2019). Such repellent factors that are expressed in the scar zone are myelin proteins of central origin Nogo, glycoproteins MAG and OMgp, type IV collagen, chondroitin sulfate proteoglycans (aggrecan, versican, neurocan, brevican and phosphacan), embryonic Wnt factor, semaphorin 3, netrin 1, ephrin B3, RGMa and RGMb factors, BMP2/4 factor, some astrocytic factors (García-Alías and Fawcett 2012, Tran *et al* 2018, Ueno *et al* 2020, Nakamura *et al* 2021). These conditions prevent local axonal cones and cell populations from migrating and regenerating. The overall regeneration capacity of the mammalian spinal cord largely depends on the presence of extracellular factors (proteoglycans, Netrin-1, Ephrin, Sema7A, EphrinB2, etc) and their specific composition (presence/absence, sufficient quantity, ratio, available form, etc) (Tran *et al* 2018, Domínguez-Romero and Slater 2021, Li *et al* 2021). When the extracellular matrix is preserved, anatomically and histologically normal tissues regenerate naturally. However, the site of injury usually undergoes compact fibroglial scar or cyst formation that complicates axonal outgrowth and regeneration, causing local spinal cord compression and impairing spinal cord function. If the majority of the extracellular matrix is lost as a result of trauma, the scar substitutes for normal tissue at the site of injury (Wang *et al* 2018).

The extracellular matrix (ECM) consists of a macromolecular network forming a gel-like hydrated structure (interstitial network) that that consists of glycosaminoglycans and proteoglycans and provides structural and functional integrity to the tissue. To be successfully used in tissue reconstruction, the biomaterial must most likely imitate or partially imitate such a matrix structure (Niemczyk *et al* 2018, Xue *et al* 2021). Interestingly, the composition and mechanical properties of the extracellular matrix affect many cellular functions, including morphogenesis, cell anchorage and survival, signaling. Various structural proteins (fibronectin, various types of collagens, laminin, elastin), growth factors, modular proteoglycans and cell surface proteoglycans, small leucine-rich proteoglycans and glycans (hyaluronic acid) are associated with ECM (Valdoz *et al* 2021). In addition, some of the components of the ECM, such as laminin, promote more neurite outgrowth, and CSPG and fibronectin inhibit neurite re-growth *in vitro*. Removal of inhibitory components of ECM, such as CSPG, improves neurite outgrowth *in vivo*, while removal of other ECM proteins, such as collagens, does not promote regeneration or repair. The stiffness and orientation of the ECM scaffolds may also act as a physical cue for neurite outgrowth, leading to strategies to align ECM components to promote directed axonal growth (Orr and Gensel 2018).

Since the extracellular matrix controls intercellular signaling, it regulates the diffusion of signaling molecules and factors required for normal tissue functioning and regeneration in cases of trauma. Understanding these processes has led to the development of two restorative surgery strategies: replacement surgery, i.e. replacing lost cells and artificial substrate implantation (Assinck *et al* 2017, Wang *et al* 2018, Cizkova *et al* 2019, Jin *et al* 2019, Liu *et al* 2019, Zhang *et al* 2019, Shah *et al* 2020, Cheng *et al* 2022, Tashiro *et al* 2022, Wang *et al* 2022). The most promising strategy for the rehabilitation of chronic SCI is the combination of these two strategies (Cizkova *et al* 2019, Wang *et al* 2022).

The first strategy relies on replacing the lost nerve cells with different types of stem, progenitor, or differentiated cells (Cizkova *et al* 2019, Jin *et al* 2019, Shah *et al* 2020, Farid *et al* 2022, Suzuki *et al* 2022). It is assumed that transplanted into the injury site, embryonic or fetal stem cell-derived neurons may

potentially grow into the injured tissue and establish a network with the recipient's cells. However, the functional significance of these contacts remains unclear. Most of the evidence suggests that the positive regenerative impact of cell transplantation is connected to pathotropic homing (Oliveri *et al* 2014, Assinck *et al* 2017), a rare *in vivo* phenomenon of neurogenic transdifferentiation (Huang *et al* 2015, Dennie *et al* 2016), the fusion of transplanted cells with recipient's tissue cells (Noiseux *et al* 2006) and effects of microvesicular (Cizkova *et al* 2019, Rohde *et al* 2019, Yin *et al* 2019), paracrine or cellular contacts (Bratton and Henson 2005, Gabryel *et al* 2012), the complex action of condition media, derived from stem cells (Cizkova *et al* 2019), and promotion of axonal growth in the area of injury. Currently, several cell types are being studied as potential transplant alternatives, such as neural stem cells of different origins, neural progenitors, neural and glial precursors, MSCs of different origins, neural crest stem cells, olfactory ensheathing cells, endothelial progenitors, oligodendrocytes, and Schwann cells (Ahuja *et al* 2017, Cizkova *et al* 2019, Jin *et al* 2019, Shah *et al* 2020, Farid *et al* 2022, Suzuki *et al* 2022). Nevertheless, clinical data suggest that transplants only slightly improve the clinical symptoms, in particular, motor function (Ahuja *et al* 2017, Dalamagkas *et al* 2018, Jin *et al* 2019) without qualitatively influencing the structural dynamics. The reasons for the decreased efficiency of such transplants include the low viability of the transplanted cells (Vismara *et al* 2017, Dalamagkas *et al* 2018), immune response initiation, and local inflammatory reactions (Praet *et al* 2015, Le Blon *et al* 2017) which often involve cytokines produced by the transplanted cells (Pajer *et al* 2014, 2015). The successful resolution of these issues would require the transplantation of a much higher number of cells (Vismara *et al* 2017), which largely restricts prospective clinical implementation. In cases of spinal cord or peripheral nerve injury, the main goal of medical intervention is the restoration of the damaged nerve fibers rather than of the neuron population (Ahuja *et al* 2017, Han *et al* 2019, Liu *et al* 2019, Zhang *et al* 2019).

The second neuroengineering strategy is the artificial matrix implantation that may be 'empty' or combined with the neurotrophic factors and/or various types of cells, whose transplantation is considered to be effective in case of the white matter or periphery nerve injury (Ghosh *et al* 2018, Guo and Ma 2018, Lu *et al* 2018, Oliveira *et al* 2018, Cizkova *et al* 2019, Liu *et al* 2019, Zhang *et al* 2019, Cheng *et al* 2022, Tashiro *et al* 2022).

Modern experimental studies have focused mainly on the efficiency of synthetic tube matrix transplants consisting of poly-acrylonitrile vinyl chloride, polycarbonates, and poly(alpha-hydroxy) acids etc (Ziemba and Gilbert 2017, Ghosh *et al* 2018, Oliveira *et al* 2018, Wang *et al* 2018, Cheng *et al* 2022). The transplantation of these substrates stimulates axonal outgrowth. In addition, a number of water-soluble substrates, such as PEG, have been suggested for use in transplantation. However, such substances usually form 2D carcasses, allowing for surrounding tissue outgrowth, but preventing these tissues from self-organizing into a 3D structure. Under such conditions, the connections between cells deteriorate and the cellular composition changes, as such polymer materials are unable to provide the same support as the lost extracellular matrix (Fouad *et al* 2009, Wang *et al* 2018).

To date, the combination of matrices with cells and/or additional factors (the third strategy) is probably the most promising strategy for rehabilitation treatment of chronic SCI (Cizkova *et al* 2019, Liu *et al* 2019, Zhang *et al* 2019, Tashiro *et al* 2022, Wang *et al* 2022).

These issues have stimulated the search for amorphous porous gel-type materials that can be transplanted effectively. Such hydrogels must possess the 3D structure of a hydrophilic polymer macromolecular network that is capable of swelling in a liquid environment (Zhu and Marchant 2011, Guvendiren and Burdick 2013). One such pHPMA derivative is NeuroGel, a biologically compatible hydrogel whose characteristic structure supports the chemically and physiologically stable environment for the recipient's cell growth when transplanted. Recent experimental data suggest that transplantation of this hydrogel in modeling both acute and chronic SCIs leads to restoration of the damaged tissue structure, making possible the germination of cell processes of the recipient's tissue. Experimental transplantation has resulted in an increase in axonal growth cone numbers and new axons (including myelinated Schwann cells) in comparison with controls; 12 months after the operation, the structure of the hydrogel changes due to the outgrowth of blood vessels and cells inside the implant; 19 months after the operation, complete myelination is observed together with deposition of collagen and fibronectin fibers and synaptogenesis, including dendritic contact formation (Woerly 2000, Woerly *et al* 2004, 2005, Gatskiy *et al* 2014). Experimental animals showed functional recovery, including quadrupedal locomotion and restoration of descending innervation through the transplanted tissue.

NeuroGel pores of varying diameters enable not only the diffusion of macromolecules, but also whole-cell migration. Such a structure allows the seeding of this hydrogel with different types of cells for possible implantation into the injury site.

The above data contributed to the development of new approaches for seeding stem cells into a heteroporous matrix hydrogel/NeuroGel. In our study, we chose direct injection of the cells into the dehydrated hydrogel and rehydration of NeuroGel in the cell suspension as the strategies for hydrogel active

or passive seeding, respectively. Murine GFP-positive BMSCs were chosen as the cell type, which allowed us to identify them in the hydrogel before and after implantation of the NeuroGel + BMSCs complex in the spinal cord. The findings demonstrated that direct injection of cells facilitated 2.5 times more cells populating the hydrogel matrix than under the conditions of the rehydration strategy (figures 3(a)–(aii)).

Studies have also demonstrated that pHPMA derivatives seeded with MSCs and implanted into the site of chronic compression SCI prevented atrophy of the tissue adjacent to the injury and improved locomotion and sensation of hind limbs in model animals 9 weeks after the operation in comparison with control animals that did not undergo transplantation and animals that received hydrogel transplant only (Hejcl *et al* 2010). The same studies also proved the effectiveness of delayed reconstructive surgery for nervous tissue regeneration, namely matrix implantation carried out after stabilization of the injured animals and not immediately after the injury occurred. These results were confirmed by other studies and should be considered when planning further experiments and clinical trials (Hejcl *et al* 2008).

When choosing the cell type for seeding and transplantation, in particular MSCs, a number of factors should be considered, based on the origin of the cells.

MSCs have been characterized for more than 30 years. According to the International Society for Cellular Therapy, the main characteristics of MSCs *in vitro*, regardless of their origin and the isolation technique, are the following: plastic adhesion (one of the easiest characteristics to detect when cells are still cultures); potency to differentiate into chondro-, osteo- and adipocytes; CD105, CD90 and CD73 surface cell marker expression; low-to-no expression of CD34, CD45, CD11 and HLA-DR markers (Rowland *et al* 2008).

Some researchers have expanded this list to include the formation of fibroblast-like colonies, whose histochemical analysis has revealed positive staining for ALP, collagen III, and fibronectin (Osipova 2011).

For our study, we chose BMSCs, as these cells are bioavailable and biosafe (in terms of clinical use, BMSCs is the most easily isolated without negative consequences for the health of the body). In addition, the properties of MSCs are best studied both experimentally and clinically during transplantation after SCI (Oliveri *et al* 2014, Bonaventura *et al* 2020, Pang *et al* 2021, 2022, Farid *et al* 2022).

MSCs transplantation (Khan *et al* 2018, Bonaventura *et al* 2020, Yousefifard *et al* 2020) in combination with a polymer matrix (Liu *et al* 2018, Wang *et al* 2018, Zhang *et al* 2019, Liu *et al* 2019) is one of the most actively studied areas of rehabilitation treatment for SCI (Farid *et al* 2022). The positive effect of MSCs in SCI is associated with pathotropic homing (Oliveri *et al* 2014), a rare *in vivo* phenomenon of neurogenic transdifferentiation (Oliveri *et al* 2014, Huang *et al* 2015, Dennie *et al* 2016), fusion with cells of the recipient tissue (Noiseux *et al* 2006), microvesicular (Cizkova *et al* 2019, Rohde *et al* 2019, Yin *et al* 2019), the influence of growth factors (Oliveri *et al* 2014) or contact exposure (Oliveri *et al* 2014), as well as with a positive effect on the course of the inflammatory process in the area of injury (Pang *et al* 2022) and scarring (Pang *et al* 2021) in general causes a positive influence on the regeneration of damaged nerve fibers of the spinal cord (Lin *et al* 2018). Many of these effects can be potentiated by MSC transplantation in combination with matrices (Lv *et al* 2021).

Despite the ongoing discussion on the neuronal differentiation ability of (Thompson *et al* 2019, Urrutia *et al* 2019, Venkatesh *et al* 2019), the results of our study suggest that BMSCs inside the hydrogel are capable of differentiating into neuronal lineage (NeuN-positive and β(III)-tubulin-positive cells), while preserving low proliferative potential (Ki-67-positive cells) (figures 3(b) and (c)). We were unable to detect statistically significant differences in BMSCs differentiation potential under different (injection and rehydration variant) co-cultivation protocols (figures 3(d) and (e)).

Interestingly, we did not use any additional chemicals to differentiate the BMSCs into neurons. Numerous *in vitro* experiments have described multiple triggers of neural differentiation in BMSCs, such as retinoid acid, growth factors (including their combinations), antioxidants, demethylating agents, compounds triggering intracellular cAMP concentration elevation, and the ontogenetic inductor Noggin (Rybachuk and Pivneva 2013, Luo *et al* 2017, Thompson *et al* 2019). Previous studies have suggested that BMSCs are capable of differentiating into neuron-like and glial cells, which was confirmed by the expression of neural markers in cells, such as—nestin, vimentin, NeuN, β(III)-tubulin, NSE, NF-M, GFAP, Gal-C, NCAM, BDNF, and glutamate (Okolicsanyi *et al* 2014, Fang *et al* 2016). Most of these *in vitro* studies have reported differentiation into both glial cells (Lei *et al* 2007, Sharma *et al* 2017) and neuron-like cells (Ma *et al* 2019, Urrutia *et al* 2019). In addition, some studies have demonstrated that differentiated cells, such as functionally mature neurons, respond to depolarizing stimuli like the functionally mature neurons (Xu *et al* 2008, Liu *et al* 2012). Some authors describe spontaneous differentiation of 50%–70% cultured MSCs into NeuN-positive and β(III)-tubulin-positive cells. Neuronal differentiation has been observed in BMSCs co-cultivated with different types of matrix—collagen with fibronectin and laminin (Lee *et al* 2011), deoxidized forms of graphene oxide (Guo *et al* 2016), polystyrene and poly-ε-caprolactone (Shirian *et al* 2016), gialuronic acid (Luo *et al* 2012), chitin nanofibers

(Shou *et al* 2018) and poly-pyrrole-alginate hydrogel (Yang *et al* 2016), and 3D conductive fibrous scaffolds of silk fibroin and reduced graphene oxide (Rahmani *et al* 2019).

Previous studies have shown high pHPMA-hydrogel biocompatibility and its close integration into injured spinal cord tissue (Woerly *et al* 1996, 1998, 1999, Woerly 2000, Woerly *et al* 2001b, 2004). A study using a silver impregnation technique (Woerly *et al* 2001b) detected nerve fiber ingrowth into a pHPMA-hydrogel implanted in the lateral hemisection area of the rat spinal cord. The ingrowth of nerve fibers into the depth of the implanted pHPMA-hydrogel was also confirmed by the immunohistochemical identification of neurofilaments (Woerly *et al* 2001a, Pertici *et al* 2013).

In an *in vivo* study, we showed posttraumatic recovery of spinal cord tissue after injury, followed by implantation of the hydrogel + BMSCs complex (approximately 7 months after injury modeling). The implant zone was closely linked to the recipient tissue (figures 5(a) and 6(b)), and the recipient cells grew freely into the hydrogel itself. In turn, within the hydrogel + BMSCs complexes themselves, a densely formed network of β(III)-tubulin-positive cells (mainly GFP cells), that is, a neuronal network (figure 6(a)), was visible.

Our results of a morphological study of damaged spinal cord tissue in rats implanted with NeuroGel + BMSCs clearly explain earlier results of functional recovery and a change in the level of staticity. The revealed morphological picture was accompanied by a tendency to improve the motor function of the paretic limb in comparison with similar implantation of an empty hydrogel (Tsymbaliuk *et al* 2016a, 2016b). In particular, when assessing the BBB scale, a significant difference in the motor function of the paretic limb was found for groups in which trauma was simulated and empty hydrogel implanted (for 2–28 weeks; $p < 0.001$), and for groups in which trauma was simulated and hydrogel with BMSCs implanted (for 1–28 weeks; $p \leqslant 0.02$), while for groups in which empty and filled with BMSCs hydrogel was implanted the maximal difference was noted on the 24th week ($p = 0.055$) (Tsymbaliuk *et al* 2016a).

Taking into consideration all the evidence confirming the positive outcome of BMSCs transplantation in the context of regenerative therapy for nervous system injury (Kandalam *et al* 2017, Liu *et al* 2018), the results of this study provide an experimental basis for further use of pHPMA hydrogel/NeuroGel-based implants populated with stem cells of different origins and their implantation into lesion sites, i.e. the spinal cord. The data from this study can enable the creation of an algorithm for choosing the most effective combination of components for implantation, reducing possible negative side effects, and facilitating the rehabilitation process.

Data availability statement

The data generated and/or analyzed during the current study are not publicly available for legal/ethical reasons but are available from the corresponding author on reasonable request.

Acknowledgments

We thanks Dr. Vitalii Kyryk for help with immunophenotyping of stem cells; Mr. Dmytro Nesterenko for participating in some stages of spinal cord tissue preparation; Prof. Volodymyr Kozyavkin for providing some reagents.

Funding statement

The work was carried out in the context of two state research projects: *Romodanov Neurosurgery* Institute NAMS of Ukraine (0113U007731) and Bogomolets National Medical University (0115U000013).

Conflict of interest

There are no conflicts of interest to declare, including any financial, personal, or other relationship with other people or organizations.

Contributors

O R and V M conceived the study, designed and performed *in vivo* experiments, and wrote the manuscript; O R designed and performed *in vitro* experiments, analyzed the data and conducted the statistics; NS helped to prepare cell cultures and preparation of spinal cord tissue for immunostaining; É P manufactured NeuroGel; YuYa provided NeuroGel. All authors discussed and commented on the manuscript.

Ethical conduct

This study was conducted in accordance with the protocols approved by the Animal Care and Use Committee at the Bogomoletz Institute of Physiology (National Acad. Sci. of Ukraine), Institute of Genetic and Regenerative Medicine M D Strazhesko National Scientific Center of Cardiology, Clinical and Regenerative Medicine (National Acad. Med. Sci. of Ukraine), *Romodanov Neurosurgery* Institute (National Acad. Med. Sci. of Ukraine), Bogomolets National Medical University and the Law of Ukraine on the Protection of Experimental Animals (N3447-IV, 21.02.2006).

ORCID iD

Oksana Rybachuk https://orcid.org/0000-0002-3843-3536

References

Ahuja C S *et al* 2017 Traumatic spinal cord injury—repair and regeneration *Clin. Neurosurg.* **80** S22–S90

Alfurhood J A, Sun H, Kabb C P, Tucker B S, Matthews J H, Luesch H and Sumerlin B S 2017 Poly(N-(2-hydroxypropyl) methacrylamide)–valproic acid conjugates as block copolymer nanocarriers *Polym. Chem.* **8** 4983–7

Assinck P, Duncan G J, Hilton B J, Plemel J R and Tetzlaff W 2017 Cell transplantation therapy for spinal cord injury *Nat. Neurosci.* **20** 637–47

Augusto-Oliveira M, Arrifano G, Malva J and Crespo-Lopez M 2019 Adult hippocampal neurogenesis in different taxonomic groups: possible functional similarities and striking controversies *Cells* **8** 125

Badner A, Siddiqui A M and Fehlings M G 2017 Spinal cord injuries: how could cell therapy help? *Expert Opin. Biol. Ther.* **17** 529–41

Becker C G, Becker T and Hugnot J-P 2018 The spinal ependymal zone as a source of endogenous repair cells across vertebrates *Prog. Neurobiol.* **170** 67–80

Bianco P, Robey P G, Saggio I and Riminucci M 2010 "Mesenchymal" stem cells in human bone marrow (skeletal stem cells): a critical discussion of their nature, identity, and significance in incurable skeletal disease *Hum. Gene Ther.* **21** 1057–66

Blesch A and Tuszynski M H 2009 Spinal cord injury: plasticity, regeneration and the challenge of translational drug development *Trends Neurosci.* **32** 41–47

Bohdanecky M, Bažilová H and Kopeček J 1974 Poly[N-(2-hydroxypropyl)methacrylamide]—II: hydrodynamic properties of dilute solutions *Eur. Polym. J.* **10** 405–10

Bonaventura G, Incontro S, Iemmolo R, La Cognata V, Barbagallo I, Costanzo E, Barcellona M L, Pellitteri R and Cavallaro S 2020 Dental mesenchymal stem cells and neuro-regeneration: a focus on spinal cord injury *Cell Tissue Res.* **379** 421–8

Bratton D L and Henson P M 2005 Autoimmunity and apoptosis: refusing to go quietly *Nat. Med.* **11** 26–27

Can A and Balci D 2011 Isolation, culture, and characterization of human umbilical cord stroma-derived mesenchymal stem cells *Methods Mol. Biol.* **698** 51–62

Cascone S and Lamberti G 2020 Hydrogel-based commercial products for biomedical applications: a review *Int. J. Pharm.* **573** 118803

Cheng Y, Zhang Y and Wu H 2022 Polymeric fibers as scaffolds for spinal cord injury: a systematic review *Front. Bioeng. Biotechnol.* **9** 807533

Cizkova D *et al* 2019 Spinal cord injury: animal models, imaging tools and the treatment strategies *Neurochem. Res.* **45** 134–43

Dalamagkas K, Tsintou M, Seifalian A and Seifalian A 2018 Translational regenerative therapies for chronic spinal cord injury *Int. J. Mol. Sci.* **19** 1776

Dennie D, Louboutin J-P and Strayer D S 2016 Migration of bone marrow progenitor cells in the adult brain of rats and rabbits *World J. Stem Cells* **8** 136–57

Dietz V and Schwab M E 2017 From the rodent spinal cord injury model to human application: promises and challenges *J. Neurotrauma* **34** 1826–30

Domínguez-Romero M E and Slater P G 2021 Unraveling axon guidance during axotomy and regeneration *Int. J. Mol. Sci.* **22** 8344

Dominici M, Le Blanc K, Mueller I, Slaper-Cortenbach I, Marini F C, Krause D S, Deans R J, Keating A, Prockop D J and Horwitz E M 2006 Minimal criteria for defining multipotent mesenchymal stromal cells. The international society for cellular therapy position statement *Cytotherapy* **8** 315–7

Fan X, Wang J-Z, Lin X-M and Zhang L 2017 Stem cell transplantation for spinal cord injury: a meta-analysis of treatment effectiveness and safety *Neural Regen. Res.* **12** 815

Fang H, Song P, Shen C, Liu X and Li H 2016 Bone mesenchymal stem cell-conditioned medium induces the upregulation of Smad6, which inhibits the BMP-4/Smad1/5/8 signaling pathway *Neurol. Res.* **38** 965–72

Farid M F, Abouelela Y S and Rizk H 2022 Stem cell treatment trials of spinal cord injuries in animals *Auton. Neurosci.* **238** 102932

Fathi M, Alami-Milani M, Geranmayeh M H, Barar J, Erfan-Niya H and Omidi Y 2019 Dual thermo-and pH-sensitive injectable hydrogels of chitosan/(poly(N-isopropylacrylamide-co-itaconic acid)) for doxorubicin delivery in breast cancer *Int. J. Biol. Macromol.* **128** 957–64

Fouad K, Pearse D D, Tetzlaff W and Vavrek R 2009 Transplantation and repair: combined cell implantation and chondroitinase delivery prevents deterioration of bladder function in rats with complete spinal cord injury *Spinal Cord* **47** 727–32

Gabryel B, Kost A and Kasprowska D 2012 Neuronal autophagy in cerebral ischemia–a potential target for neuroprotective strategies? *Pharmacol. Rep.* **64** 1–15

García-Alías G and Fawcett J W 2012 Training and anti-CSPG combination therapy for spinal cord injury *Exp. Neurol.* **235** 26–32

Gatskiy A A, Tretyak I B and Tsymbaliuk V 2014 Biocompatible heterogeneous porous gel matrix NeuroGel(TM) promotes regeneration of rat sciatic nerve within tubular silicone prosthesis (experimental study) *Acta Neurochir.* **156** 1591–8

Ghosh B, Wang Z, Nong J, Urban M W, Zhang Z, Trovillion V A, Wright M C, Zhong Y and Lepore A C 2018 Local BDNF delivery to the injured cervical spinal cord using an engineered hydrogel enhances diaphragmatic respiratory function *J. Neurosci.* **38** 5982–95

Guo B and Ma P X 2018 Conducting polymers for tissue engineering *Biomacromolecules* **19** 1764–82

Guo W, Wang S, Yu X, Qiu J, Li J, Tang W, Li Z, Mou X, Liu H and Wang Z 2016 Construction of a 3D rGO–collagen hybrid scaffold for enhancement of the neural differentiation of mesenchymal stem cells *Nanoscale* **8** 1897–904

Guvendiren M and Burdick J A 2013 Engineering synthetic hydrogel microenvironments to instruct stem cells *Curr. Opin. Biotechnol.* **24** 841–6

Han G H *et al* 2019 Therapeutic strategies for peripheral nerve injury: decellularized nerve conduits and Schwann cell transplantation *Neural Regen. Res.* **14** 1343–51

Hejcl A *et al* 2010 HPMA-RGD hydrogels seeded with mesenchymal stem cells improve functional outcome in chronic spinal cord injury *Stem Cells Dev.* **19** 1535–46

Hejcl A, Lesný P, Přádný M, Michálek J, Jendelová P, Štulík J and Syková E 2008 Biocompatible hydrogels in spinal cord injury repair *Physiol. Res.* **57** S121–32

Huang B, Li G and Jiang X H 2015 Fate determination in mesenchymal stem cells: a perspective from histone-modifying enzymes *Stem Cell Res. Ther.* **6** 35

Jin M C, Medress Z A, Azad T D, Doulames V M and Veeravagu A 2019 Stem cell therapies for acute spinal cord injury in humans: a review *Neurosurg. Focus* **46** E10

Kandalam S *et al* 2017 Pharmacologically active microcarriers delivering BDNF within a hydrogel: novel strategy for human bone marrow-derived stem cells neural/neuronal differentiation guidance and therapeutic secretome enhancement *Acta Biomater.* **49** 167–80

Khan S, Mafi P, Mafi R and Khan W 2018 A systematic review of mesenchymal stem cells in spinal cord injury, intervertebral disc repair and spinal fusion *Curr. Stem Cell Res. Ther.* **13** 316–23

Khorasanizadeh M *et al* 2019 Neurological recovery following traumatic spinal cord injury: a systematic review and meta-analysis *J. Neurosurg. Spine* **30** 683–99

Kopach O, Medvediev V, Krotov V, Borisyuk A, Tsymbaliuk V and Voitenko N 2017 Opposite, bidirectional shifts in excitation and inhibition in specific types of dorsal horn interneurons are associated with spasticity and pain post-SCI *Sci. Rep.* **7** 5884

Kopeček J and Bažilová H 1973 Poly[N-(2-hydroxypropyl) methacrylamide]—I. Radical polymerization and copolymerization *Eur. Polym. J.* **9** 7–14

Kopecék J and Baźilová H 1974 Poly[N-(2-hydroxypropyl) methacrylamide]—iii: crosslinking copolymerization *Eur. Polym. J.* **10** 465–70

Kopecek J and Kopecková P 2010 HPMA copolymers: origins, early developments, present, and future *Adv. Drug Deliv. Rev.* **62** 122–49

Le Blon D, Hoornaert C, Detrez J R, Bevers S, Daans J, Goossens H, De Vos W H, Berneman Z and Ponsaerts P 2017 Immune remodelling of stromal cell grafts in the central nervous system: therapeutic inflammation or (harmless) side-effect? *J. Tissue Eng. Regen. Med.* **11** 2846–52

Lee J H, Yu H-S, Lee G-S, Ji A, Hyun J K and Kim H-W 2011 Collagen gel three-dimensional matrices combined with adhesive proteins stimulate neuronal differentiation of mesenchymal stem cells *J. R. Soc. Interface* **8** 998–1010

Lei Z, Yongda L, Jun M, Yingyu S, Shaoju Z, Xinwen Z and Mingxue Z 2007 Culture and neural differentiation of rat bone marrow mesenchymal stem cells *in vitro Cell Biol. Int.* **31** 916–23

Li J, Mareddy S, Tan D M, Crawford R, Long X, Miao X and Xiao Y 2009 A minimal common osteochondrocytic differentiation medium for the osteogenic and chondrogenic differentiation of bone marrow stromal cells in the construction of osteochondral graft *Tissue Eng.* A **15** 2481–90

Li X *et al* 2019 Aligned scaffolds with biomolecular gradients for regenerative medicine *Polymers* **11** 341

Li Z, Yu S, Hu X, Li Y, You X, Tian D, Cheng L, Zheng M and Jing J 2021 Fibrotic scar after spinal cord injury: crosstalk with other cells, cellular origin, function, and mechanism *Front. Cell Neurosci.* **15** 720938

Lin L, Lin H, Bai S, Zheng L and Zhang X 2018 Bone marrow mesenchymal stem cells (BMSCs) improved functional recovery of spinal cord injury partly by promoting axonal regeneration *Neurochem. Int.* **115** 80–84

Liu J, Song L, Jiang C, Liu Y, George J, Ye H and Cui Z 2012 Electrophysiological properties and synaptic function of mesenchymal stem cells during neurogenic differentiation—a mini-review *Int. J. Artif. Organs* **35** 323–37

Liu S, Schackel T, Weidner N and Puttagunta R 2018 Biomaterial-supported cell transplantation treatments for spinal cord injury: challenges and perspectives *Front. Cell Neurosci.* **11** 430

Liu S, Xie Y-Y and Wang B 2019 Role and prospects of regenerative biomaterials in the repair of spinal cord injury *Neural Regen. Res.* **14** 1352–63

Lu P, Ceto S, Wang Y, Graham L, Wu D, Kumamaru H, Staufenberg E and Tuszynski M H 2017 Prolonged human neural stem cell maturation supports recovery in injured rodent CNS *J. Clin. Invest.* **127** 3287–99

Lu X, Perera T H, Aria A B and Smith Callahan L A 2018 Polyethylene glycol in spinal cord injury repair: a critical review *J. Exp. Pharmacol.* **10** 37–49

Luo F, Zhou D, He L, Wu J-H, Ding Q-F, Zhang J, Li Y and Zhou M-K 2012 Effect of hyaluronic acid on promoting bone marrow-derived mesenchymal stem cells to differentiate into neural cells *in vitro Sichuan Da Xue Xue Bao Yi Xue Ban* **43** 352–7

Luo H *et al* 2017 Neural differentiation of bone marrow mesenchymal stem cells with human brain-derived neurotrophic factor gene-modified in functionalized self-assembling peptide hydrogel *in vitro J. Cell. Biochem.* **119** 1420–8

Lv B, Zhang X, Yuan J, Chen Y, Ding H, Cao X and Huang A 2021 Biomaterial-supported MSC transplantation enhances cell–cell communication for spinal cord injury *Stem Cell Res. Ther.* **12** 36

Lv Z, Dong C, Zhang T and Zhang S 2022 Hydrogels in spinal cord injury repair: a review *Front. Bioeng. Biotechnol.* **10** 931800

Ma Y, Ma J, Zhao Y, Yang K, Zhou J, Gao F, Pan R and Lu G 2019 Comparison of phenotypic markers and neural differentiation potential of human bone marrow stromal cells from the cranial bone and iliac crest *J. Cell. Physiol.* **234** 15235–42

Matsuda C, Takagi M, Hattori T, Wakitani S and Yoshida T 2005 Differentiation of human bone marrow mesenchymal stem cells to chondrocytes for construction of three-dimensional cartilage tissue *Cytotechnology* **47** 11–17

Medvediev V V *et al* 2021 Model of spinal cord lateral hemi-excision at the lower thoracic level for the tasks of reconstructive and experimental neurosurgery *Ukr. Neurosurg. J.* **27** 33–53

Mohapatra S *et al* 2021 Regulatory updates on hydrogel: an extensive review pp 1–32

Myers S A *et al* 2016 Does the preclinical evidence for functional remyelination following myelinating cell engraftment into the injured spinal cord support progression to clinical trials? *Exp. Neurol.* **283** 560–72

Nakamura Y, Ueno M, Niehaus J K, Lang R A, Zheng Y and Yoshida Y 2021 Modulation of both intrinsic and extrinsic factors additively promotes rewiring of corticospinal circuits after spinal cord injury *J. Neurosci.* **41** 10247–60

Niemczyk B, Sajkiewicz P and Kolbuk. D 2018 Injectable hydrogels as novel materials for central nervous system regeneration *J. Neural Eng.* **15** 051002

Nishio T, Fujiwara H and Kanno I 2018 Immediate elimination of injured white matter tissue achieves a rapid axonal growth across the severed spinal cord in adult rats *Neurosci. Res.* **131** 19–29

Noiseux N, Gnecchi M, Lopez-Ilasaca M, Zhang L, Solomon S D, Deb A, Dzau V J and Pratt R E 2006 Mesenchymal stem cells overexpressing Akt dramatically repair infarcted myocardium and improve cardiac function despite infrequent cellular fusion or differentiation *Mol. Ther.* **14** 840–50

Nori S, Nakamura M and Okano H 2017 Plasticity and regeneration in the injured spinal cord after cell transplantation therapy *Prog. Brain Res.* **231** 33–56

Obernier K and Alvarez-Buylla A 2019 Neural stem cells: origin, heterogeneity and regulation in the adult mammalian brain *Development* **146** dev156059

Okolicsanyi R K, Griffiths L R and Haupt L M 2014 Mesenchymal stem cells, neural lineage potential, heparan sulfate proteoglycans and the matrix *Dev. Biol.* **388** 1–10

Oliveira J M *et al* 2018 Hydrogel-based scaffolds to support intrathecal stem cell transplantation as a gateway to the spinal cord: clinical needs, biomaterials, and imaging technologies *npj Regen. Med.* **3** 8

Oliveri R S, Bello S and Biering-Sørensen F 2014 Mesenchymal stem cells improve locomotor recovery in traumatic spinal cord injury: systematic review with meta-analyses of rat models *Neurobiol. Dis.* **62** 338–53

Ooi Y Y, Ramasamy R and Vidyadaran S 2008 Mouse bone marrow mesenchymal stem cells acquire CD45-CD106+ immunophenotype only at later passages *Med. J. Malaysia* **63** 65–66

Orr M B and Gensel J C 2018 Spinal cord injury scarring and inflammation: therapies targeting glial and inflammatory responses introduction: glial effectors of spinal cord injury scarring and inflammation *Neurotherapeutics* **15** 1–13

Osipova E 2011 Biological characteristics of mesenchymal stem cells during ex vivo expansion *Br. J. Med. Med. Res.* **1** 85–95

Pajer K *et al* 2014 Cytokine signaling by grafted neuroectodermal stem cells rescues motoneurons destined to die *Exp. Neurol.* **261** 180–9

Pajer K et al 2015 Grafted murine induced pluripotent stem cells prevent death of injured rat motoneurons otherwise destined to die *Exp. Neurol.* **269** 188–201
Pang Q M et al 2021 Neuroinflammation and scarring after spinal cord injury: therapeutic roles of MSCs on inflammation and glial scar *Front. Immunol.* **12** 1–14
Pang Q M et al 2022 Regulatory role of mesenchymal stem cells on secondary inflammation in spinal cord injury *J. Inflamm Res.* **15** 573–93
Pertici V et al 2013 The use of poly(N-[2-hydroxypropyl]-methacrylamide) hydrogel to repair a T10 spinal cord hemisection in rat: a behavioural, electrophysiological and anatomical examination *ASN Neuro* **5** 149–66
Praet J et al 2015 Early inflammatory responses following cell grafting in the CNS trigger activation of the subventricular zone: a proposed model of sequential cellular events *Cell Transplant.* **24** 1481–92
Qu J, Zhao X, Ma P X and Guo B 2017 pH-responsive self-healing injectable hydrogel based on N-carboxyethyl chitosan for hepatocellular carcinoma therapy *Acta Biomater.* **58** 168–80
Rahmani A et al 2019 Conductive electrospun scaffolds with electrical stimulation for neural differentiation of conjunctiva mesenchymal stem cells *Artif. Organs* 43 780–90
Říhová B, Kopeček J, Ulbrich K and Chytrý V, 1985 Immunogenicity of N-(2-hydroxypropyl) methacrylamide copolymers *Die Makromol. Chemie* **9** 13–24
Rohde E, Pachler K and Gimona M 2019 Manufacturing and characterization of extracellular vesicles from umbilical cord–derived mesenchymal stromal cells for clinical testing *Cytotherapy* **21** 581–92
Rowland J W, Hawryluk G W J, Kwon B and Fehlings M G 2008 Current status of acute spinal cord injury pathophysiology and emerging therapies: promise on the horizon *Neurosurg. Focus* **25** E2
Rustagi T and Lavelle W F 2014 Spontaneous resolution of cervical cord compression induced by hydrogel (Duraseal) *Spine J.* **14** 2511–2
Rybachuk O A and Pivneva T A 2013 Prospects of the use of mesenchymal and neuromesenchymal stem cells *Neurophysiology* **45** 477–94
Shah M, Peterson C, Yilmaz E, Halalmeh D R and Moisi M 2020 Current advancements in the management of spinal cord injury: a comprehensive review of literature *Surg. Neurol. Int.* **11** 1–7
Sharma A D et al 2017 Proteomic analysis of mesenchymal to Schwann cell transdifferentiation *J. Proteomics* **165** 93–101
Sharma A, Faubion W A and Dietz A B 2019 Regenerative materials for surgical reconstruction: current spectrum of materials and a proposed method for classification *Mayo Clin. Proc.* **94** 2099–116
Shirian S et al 2016 Comparison of capability of human bone marrow mesenchymal stem cells and endometrial stem cells to differentiate into motor neurons on electrospun poly(ε-caprolactone) scaffold *Mol. Neurobiol.* **53** 5278–87
Shou K et al 2018 Induction of mesenchymal stem cell differentiation in the absence of soluble inducer for cutaneous wound regeneration by a chitin nanofiber-based hydrogel. *J. Tissue Eng. Regen. Med.* **12** e867–80
Snyder J S 2019 Recalibrating the relevance of adult neurogenesis *Trends Neurosci.* **42** 164–78
Sprincl L, Exner J, Sterba O and Kopecek J 1976 New types of synthetic infusion solutions. III. Elimination and retention of poly-[N-(2-hydroxypropyl)methacrylamide] in a test organism *J. Biomed. Mater. Res.* **10** 953–63
Suzuki H, Imajo Y, Funaba M, Nishida N, Sakamoto T and Sakai T 2022 Current concepts of neural stem/progenitor cell therapy for chronic spinal cord injury *Front. Cell Neurosci.* **15** 794692
Swieck K, Conta-Steencken A, Middleton F A, Siebert J R, Osterhout D J and Stelzner D J 2019 Effect of lesion proximity on the regenerative response of long descending propriospinal neurons after spinal transection injury *BMC Neurosci.* **20** 1–20
Tashiro S, Nakamura M and Okano H 2022 Regenerative rehabilitation and stem cell therapy targeting chronic spinal cord injury: a review of preclinical studies *Cells* **11** 685
Tetzlaff W et al 2011 A systematic review of cellular transplantation therapies for spinal cord injury *J. Neurotrauma* **28** 1611–82
Thompson R, Casali C and Chan C 2019 Forskolin and IBMX induce neural transdifferentiation of MSCs through downregulation of the NRSF *Sci. Rep.* **9** 2969
Tran A P, Warren P M and Silver J 2018 The biology of regeneration failure and success after spinal cord injury *Physiol. Rev.* **98** 881–917
Tsymbaliuk V I et al 2016a The effect of implantation of NEUROGELTM used with xenogenic bone marrow stem cells on motor function recovery after experimental spinal cord injury *Int. Neurolog. J.* **6** 13–19
Tsymbaliuk V I et al 2016b The effect of NEUROGELTM used with bone marrow stem cells implantation on the course of the spasticity syndrome after experimental spinal cord injury *Int. Neurolog. J.* **7** 20–26
Ueno M et al 2020 Olig2-induced semaphorin expression drives corticospinal axon retraction after spinal cord injury *Cereb. Cortex* **30** 5702–16
Urrutia D N et al 2019 Comparative study of the neural differentiation capacity of mesenchymal stromal cells from different tissue sources: an approach for their use in neural regeneration therapies *PLoS One* **14** 1–17
Valdoz J C et al 2021 The ECM: to scaffold, or not to scaffold, that is the question *Int. J. Mol. Sci.* **22** 12690
Venkatesh K, Kumari A and Sen D 2019 MicroRNA signature changes during induction of neural stem cells from human mesenchymal stem cells *Nanomed. Nanotechnol. Biol. Med.* **17** 94–105
Verstappen K et al 2022 Systematic evaluation of spinal cord injury animal models in the field of biomaterials *Tissue Eng.* B **28** 1–11
Vismara I, Papa S, Rossi F, Forloni G and Veglianese P 2017 Current options for cell therapy in spinal cord injury *Trends Mol. Med.* **23** 831–49
Wang Y, Lv H-Q, Chao X, Xu W-X, Liu Y, Ling G-X and Zhang P 2022 Multimodal therapy strategies based on hydrogels for the repair of spinal cord injury *Mil. Med. Res.* **9** 16
Wang Y, Tan H and Hui X 2018 Biomaterial scaffolds in regenerative therapy of the central nervous system *Biomed. Res. Int.* **2018** 7848901
Woerly S et al 1998 Heterogeneous PHPMA hydrogels for tissue repair and axonal regeneration in the injured spinal cord *J. Biomater. Sci. Polym. Ed.* **9** 681–711
Woerly S 2000 Restorative surgery of the central nervous system by means of tissue engineering using NeuroGel implants *Neurosurg. Rev.* **23** 59–77
Woerly S et al 2001b Spinal cord repair with PHPMA hydrogel containing RGD peptides (NeuroGel^{TM}) *Biomaterials* **22** 1095–111
Woerly S et al 2005 Expression of heat shock protein (HSP)-25 and HSP-32 in the rat spinal cord reconstructed with Neurogel *Neurochem. Res.* **30** 721–35
Woerly S, Doan V D, Sosa N, de Vellis J and Espinosa-Jeffrey A 2004 Prevention of gliotic scar formation by NeuroGel^{TM} allows partial endogenous repair of transected cat spinal cord *J. Neurosci. Res.* **75** 262–72
Woerly S, Doan V D, Sosa N, Vellis J and Espinosa A 2001a Reconstruction of the transected cat spinal cord following NeuroGel^{TM} implantation: axonal tracing, immunohistochemical and ultrastructural studies *Int. J. Dev. Neurosci.* **19** 63–83
Woerly S, Petrov P, Syková E, Roitbak T, Simonová Z and Harvey A R 1999 Neural tissue formation within porous hydrogels implanted in brain and spinal cord lesions:

ultrastructural, immunohistochemical, and diffusion studies *Tissue Eng.* **5** 467–88

Woerly S, Plant G W and Harvey A R 1996 Cultured rat neuronal and glial cells entrapped within hydrogel polymer matrices: a potential tool for neural tissue replacement *Neurosci. Lett.* **205** 197–201

Woerly S, Ulbrich K, Chytrý V, Smetana K, Petrovický P, Říhová B and Morassutti D J 1993 Synthetic Polymer Matrices for Neural Cell Transplantation *Cell Transplant* **2** 229–39

Xie B *et al* 2015 An injectable thermosensitive polymeric hydrogel for sustained release of Avastin1 to treat posterior segment disease *Int. J. Pharm.* **490** 375–83

Xu R *et al* 2008 Functional analysis of neuron-like cells differentiated from neural stem cells derived from bone marrow stroma cells *in vitro Cell. Mol. Neurobiol.* **28** 545–58

Xue W, Shi W, Kong Y, Kuss M and Duan B 2021 Anisotropic scaffolds for peripheral nerve and spinal cord regeneration *Bioactive Mater.* **6** 4141–60

Yang S, Jang L, Kim S, Yang J, Yang K, Cho S-W and Lee J Y 2016 Polypyrrole/alginate hybrid hydrogels: electrically conductive and soft biomaterials for human mesenchymal stem cell culture and potential neural tissue engineering applications *Macromol. Biosci.* **16** 1653–61

Yin K, Wang S and Zhao R C 2019 Exosomes from mesenchymal stem/stromal cells: a new therapeutic paradigm *Biomarker Res.* **7** 8

Yousefifard M *et al* 2020 A combination of mesenchymal stem cells and scaffolds promotes motor functional recovery in spinal cord injury: a systematic review and meta-analysis *J. Neurosurg. Spine* **32** 269–84

Yu B and Gu X 2018 Combination of biomaterial transplantation and genetic enhancement of intrinsic growth capacities to promote CNS axon regeneration after spinal cord injury *Front. Med.* **13** 131–7

Zhang D and He X 2014 A meta-analysis of the motion function through the therapy of spinal cord injury with intravenous transplantation of bone marrow mesenchymal stem cells in rats *PLoS One* **9** e93487

Zhang Q, Shi B, Ding J, Yan L, Thawani J P, Fu C and Chen X 2019 Polymer scaffolds facilitate spinal cord injury repair *Acta Biomater.* **88** 57–77

Zhu J and Marchant R E 2011 Design properties of hydrogel tissue-engineering scaffolds *Expert Rev. Med. Devices* **8** 607–26

Ziemba A M and Gilbert R J 2017 Biomaterials for local, controlled drug delivery to the injured spinal cord *Front. Pharmacol.* **8** 1–20